Proceedings of the 2000 IEEE
International Conference on Robotics & Automation
San Francisco, CA • April 2000

Event-Driven Parts' Moving in 2D Endogeneous Environments

C. Serkan Karagöz[†], H. Işıl Bozma[†] & Daniel E. Koditschek[‡]

[†]Intelligent Systems Laboratory, Department of Electric and Electronic Engineering
Boğaziçi University, Bebek 80815 Istanbul Turkey

[‡]Artificial Intelligence Laboratory, EECS Department
College of Engineering, The University of Michigan, Ann Arbor, MI 48109 USA

Abstract

This paper is concerned with the parts' moving problem based on an event-driven planning and control. We are interested in developing feedback based approaches to the automatic generation of actuator commands that cause the robot to move a set of parts from an arbitrary initial disassembled configuration to a specified final configuration. In the Phase 1 of this project, a composite algorithm that reactively switches between different feedback controllers has been shown to induce a noncooperative game being played among the parts being manipulated. This paper describes experimental results with EDAR - Event-Driven Assembler Robot - developed for moving parts based on feedback techniques.

1. Introduction

We are interested in automatic generation of event based controllers that accomplish abstractly specified high level goals. In this paper we focus on the class of problems depicted in Figure 6 wherein a robot equipped with a "perfect" sensor is confronted with a "picture" of some desired final configuration of parts. Candidate solutions must generate automatically a family of sensor based feedback laws (e.g., equation (1) of Section 3) along with a logical mechanism for switching between them (e.g., Figure 4) in such a fashion that every initial configuration of the parts is guaranteed to be brought to the desired goal. We introduce a controls generator that adapts a global artificial potential function [11] for all the moveable components [5] to the situation of Figure 2, wherein there is only one actuated mechanism - the robot - that determines what, how, when and where to move all of the otherwise immobile objects. This approach represents a generalization to a two dimensional workspace of the transition from "exogenous" [10] to "endogenous" [14] versions of the one dimensional assembly problem.

The present paper reports on the results of a series of laboratory experiments with a robotic system, EDAR, depicted in Figure 1 that implements the two dimensional endogenous assembly controller [14]. In contrast to the one dimensional setting, we have as yet correctness proofs for neither the "exogenous" [5] nor "endogenous" (Figure 2) versions of this seemingly similarly elementary 2 dimensional setting. Simulation evidence for the efficacy of the feedback laws (e.g., equation (1) of Section 3) is compelling [5,8]. In contrast, a working physical setup seems to represent the only satisfactory means of assessing the efficacy of the hybrid switching rules (e.g., Figure 4), in the physical world.

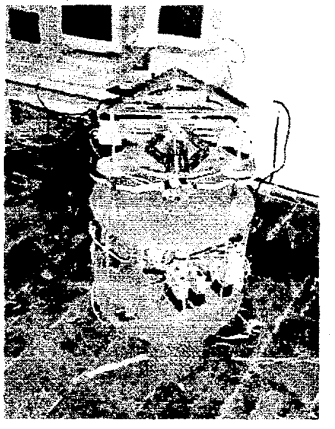

Figure 1 EDAR.

After describing the problem a little more carefully and reviewing the related literature, we describe the experimental setting in Section 2. Next, in Section 3, we review the details of the control generation scheme to be tested. Statistics from the laboratory experiments are reported in Section 4, and we conclude with a short summary of these results in Section 5.

1.1. Problem Setting

Consider a two-dimensional workspace in which a set of disk-shaped parts and a disk-shaped robot are all located at

arbitrary non-overlapping initial positions as seen in Figure 2. The parts are unactuated and cannot move unless gripped and moved by the robot. The robot can sense the position of the parts. The coarse nature of part shape presumed here to avoid introducing the rotational component of the ambient workspace is an onerous consequence of the present limits on available navigation functions [11]. Real world application of such simply represented part shapes would be limited to tasks such as arranging warehouses, packing, moving furniture and electronic component assembly.

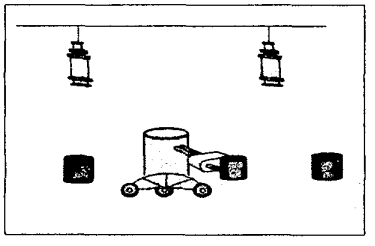

Figure 2 Problem Setting.

1.2. Related Literature

In contrast, the contemporary parts' moving literature addresses parts with very complex geometry but seems limited in scope to open-loop planning [15]. Of course, plans can result in impressive behavior when the world's true structure conforms to the rigid expectations of the planner [16]. But robot motion planners designed with this open loop perspective must always be supplemented by checks and exception handlers when implemented in the real setting. For example, ABB IRB robot [17] handles pallets, picks up boxes and places them individually. Motoman SP100 robot [18] services pallet stations and has a high-speed and high-load capacity. FANUC robot [19] achieves palletizing tasks that it handles multiple products on a single line and palletize mixed batches of products as a regular part of production. In all these systems, the execution time sensory checks and exceptions introduce an effective closed-loop mode of operation whose behavior in practice is poorly understood at best.

To summarize, the literature offers advances in mating of parts with very complex geometry - yet little provision is made regarding ensured completion of the task. Our attention is focused exactly on this latter aspect of the problem. Our technology for addressing geometric complexity is presently quite limited. We focus on ensuring convergence of the final assembly from arbitrary initial configurations, handling the inevitable execution time perturbations along the way with no additional need for exception handlers.

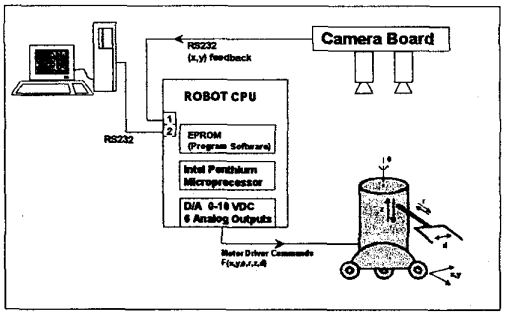

Figure 3 Robot components.

2. Robot Description

EDAR is a reaction-driven assembler robot 2D motion capabilities with an auto-blocking and a retractible arm+gripper mechanism. Figure 3 depicts the major components of EDAR. The components can be categorized into five subsystems: mechanical, electro-mechanical, electronics, vision and the control software.

2.1. Mechanical Subsystem

EDAR is a two degree of freedom mobile robot with a three degree of freedom arm and a gripper. With its arm fully retracted, the robot's orthographic projection as viewed from above is a circle 600 mm in diameter. Its mechanical design is such that without actuation, motions are irreversible. The lower plate of EDAR enables two-dimensional linear and rotational motion. There are three wheels - all of the same size and having identical wheel carriers. One DC motor actuates a mechanism that the linear motion of each of the three wheels - equal in amount - is achieved. One DC motor is used to rotate the wheels simultaneously. The arm is mounted on 600 mm. diameter steel circular plate that is stacked above the base. One DC motor rotates the upper circular plate that carries the arm mechanism, enabling around the robot shaft. One DC motor actuates a triangle shaped steel lift that locates the arm of EDAR. One DC motor actuates a prismatic mechanism to realize the radial motion of the arm. One step motor actuates two rails that carry the holders of the robot and they either move towards/away each other to grasp/ungrasp the target object.

2.2. Electro-Mechanical Design

The electro-mechanical subsystem design includes motors and their encoders, drivers and power supply. EDAR has six motors. Five of them are DC torque motors and one

motor is a step motor. These motors in conjunction with our mechanical design enable smooth acceleration/deceleration with very low backlash. The electronic subsystem includes an off the shelf PC 104 form factor board set (Pentium PRO C, D/A converter and counters). The C-coded software (including the entire motion planning algorithm as well as visual feedback and motor command loops) runs on the 2 MB processor board eprom of the processor board.

2.3. Vision System

A camera system will be interfaced to EDAR to update the position and velocity information in the robot workspace. This system is installed and programmed by another workgroup and will be integrated to EDAR. Visual processing is done on the Smarteye Vision System which is designed around a high performance DSP chip MS320C31PQL [9]. Visual feedback is generated where a camera - located exactly above the parts' moving workspace - views the cylindrical shaped objects orthographically. Our visual processing is based on selective vision concepts [13]. In our system, instead of processing the whole image, only areas around "interesting" points are fixated upon and are subjected to analysis[12].

3. Control - Endogenous Parts' Moving

In this section, we summarize our event-driven approach to parts' moving developed in [8]. Let $r=[x_r y_r]^T$ and ρ_r ($x_r, y_r \in R$ and $\rho_r \in R^+$) denote EDAR's position and its radius respectively. Each part i is uniquely specified by its position vector $p_i=[x_{pi} y_{pi}]^T$, its radius ρ_{pi}, and its destination position $d_i=[x_{di} y_{di}]^T$, $x_{pi}, y_{pi}, x_{di}, y_{di} \in R$ and $\rho_{pi} \in R^+$. A collision is specified via defining an obstacle space $O=\beta^{-1}[-\infty,0]$ where $\beta: N \to R$. The control law of the robot is as follows:

$$p(k+1)=f(p(k),u(p(k)))$$

where p is the position vector $p=\{p_i\}_{i=1,N}$ and k denotes the each subparts' moving iteration. Here, f is a mapping from the present configuration of the parts to the new world configuration after EDAR's next subparts' moving attempt. u is the feedback term and consists of two functions: next-part choice function c and motion sequence of EDAR consisting of mating to the next-part and moving it:

$$u(p(k))=u(c(k), p_{c(k)}(k+1)).$$

For each part i define a potential function $\varphi(r, p_i, \bar{p}_i)$ where $\bar{p}_i=(p_1,\ldots,p_{i-1},p_{i+1},\ldots,p_N)$. The dynamical system governing the moving of the i[th] part - which we refer to as a subassembly in the sequel - is defined via constructing a gradient vector field as:

$$\dot{p}_i=-D_{\varphi_i}\varphi_i(r,p_i,\bar{p}_i) \quad (1)$$

Let $v_i^t(r, p_i, \bar{p}_i)$ be the curve of p_i starting from the initial position $p_i(0)$. Thus, the part's position after its subassembly is defined by:

$$p_{c(k)}(k+1)=\lim_{t\to\infty} v_{c(k)}^t(r, p_i, \bar{p}_i).$$

Here, v_i^∞ represents an equilibrium configuration attained at the end of the respective subassembly. This equilibrium configuration corresponds to either the destination point of part i or an intermediate configuration that corresponds to a more suitable configuration - a better workspace geometry - for the global goal task. The resulting dynamical system which corresponds to a *game* is as follows:

$$f(p(k),u)_i=\begin{cases} u(i,p_i(k)) & if \quad i=c(k) \\ p_i(k) & otherwise \end{cases}$$

Here, the players of the game are the parts $p=\{p_i\}_{i=1,N}$ and each part i has the pay-off function φ_i which is minimum at the solution of the game.

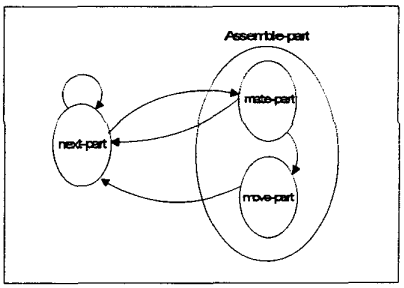

Figure 4 Subassembly Automata.

3.1. Parts' Moving as a Noncooperative Game

The parts' moving proceeds as a continual sequence of subassembly attempts - invoked repetitiously until the parts' moving is completely realized as shown in Figure 4. Each subassembly consists of i) next-part: deciding next part to be moved, ii) mate-part: robot mates with the

designated part, iii) move-part: carrying the part towards its destination. Each of the mate-part and move-part stages is realized via the use of a family of the feedback controllers that will provide the robot actuations of the respective stages. The construction of the feedback controllers is motivated by navigation functions.

3.2. Sub-goal: Next-Part

The next-part choice function c determines the next-part to be subassembled based on optimizing three criteria:
i) The distance between the corresponding part and its desired location:

$$c_1(p_i) = (x_{pi} - x_{di})^2 + (y_{pi} - y_{di})^2,$$

ii) The distance of EDAR to the part:

$$c_2(p_i) = (x_r - x_{pi})^2 + (y_r - y_{pi})^2,$$

iii) "The population" of the remaining parts around the corresponding part:

$$c_3(p_i) = \prod_{j=1, j\neq i}^{N} \left[(x_{pj} - x_{pi})^2 + (y_{pj} - y_{pi})^2 - (\rho_{pj} + \rho_{pi})^2\right]$$

EDAR chooses the part according to:

$$c = \max_j \left\{c_1(p_j) c_2(p_j) c_3(p_j)\right\}.$$

3.3. Sub-goal: Mate-Part

Mating with a part turns out to be a straightforward navigation problem among ellipsoid objects. The corresponding navigation function is: $\varphi_{mate}(p_m) = \dfrac{\alpha(m)^k}{\beta(m)}$ where $\alpha(m)$ and obstacle function $\beta(m)$ are defined as follows:

$$\alpha(m) = (x_r - x_{pm})^2 + (y_r - y_{pm})^2$$

$$\beta(m) = \prod_{i=1}^{N} \left[(x_r - x_{pi})^2 + (y_r - y_{pi})^2 - (\rho_r + \rho_{pi})^2\right]$$

k is a compensation factor.

3.4. Sub-goal: Move-Part

Once mated, the resulting robot+part pair changes the workspace topology as shown in Figure 5. Thus, the obstacle function is formulated taking this into account. If m denotes the grasped part, the control law is defined based on $\varphi_{move}(p_m) = \dfrac{\alpha^k(m)}{\beta(m)}$ where $\alpha(m)$ and $\beta(m)$ are given as follows:

$$\alpha(m) = (x_{pm} - x_{dm})^2 + (y_{pm} - y_{dm})^2$$

$$\beta(m) = \prod_{i=1, i\neq m}^{N} \left[(x_r - x_{pi})^2 + (y_r - y_{pi})^2 - (\rho_r + \rho_{pi})^2\right] \prod_{i=1, i\neq m}^{N} \left[(x_{pm} - x_{pi})^2 + (y_{pm} - y_{pi})^2 - (\rho_{pm} + \rho_{pi})^2\right]$$

Since the robot and the part are coupled and the equations of motion are calculated with respect to robot dynamics, p_m is transformed to robot coordinates r. This transformation is defined as:

$$x_{pm} = x_r + l\cos\theta$$

$$y_{pm} = y_r + l\sin\theta$$

where l and θ is the radial/angular distance between their centers respectively.

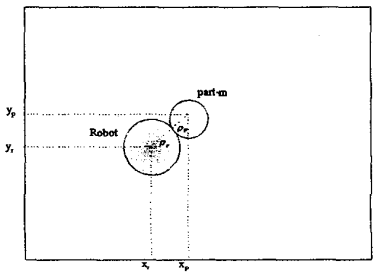

Figure 5 EDAR is mating with part m.

4. Experimental Results

In this Section, we offer statistical performance evaluation of EDAR in a series of experiments in the style originally introduced in [5]. Due to restricted physical workspace dimensions we limit our experiments to two cylindrical objects, varying from 15 cm. to 25 cm. in diameter. The 2-part assembly configurations used in experiments are as graphically shown in Figure 6. Here, EDAR is the black solid circle. The parts are on their initial positions and they are represented by the numbered circles. The destinations of the parts are indicated by the small circles. We consider four randomly chosen final configurations of increasing difficulty as shown in Figure 6. The workspace complexity measure *erc* is defined as follows:

$$erc = \frac{\|p_1(0) - d_1\|}{\|p_1(0) - d_2\|} \frac{\|p_2(0) - d_2\|}{\|p_2(0) - d_1\|}$$

where $p_i(0)$ represents the initial position of ith part and d_i is the destination vector of the ith part. The configuration at the top-left figure is a simple workspace configuration where both of the parts are initially close to

their respective destinations. At the bottom right one, the parts' moving is relatively more complex as each part is initially closer to the other part's destination - so there is a certain amount of blocking each other. In the graphs, each data point represents the mean and the deviation of 5 runs with random initial configurations. In the experiments, the camera system is not used and the initial coordinates of the parts and EDAR initial position are given as the input to EDAR.

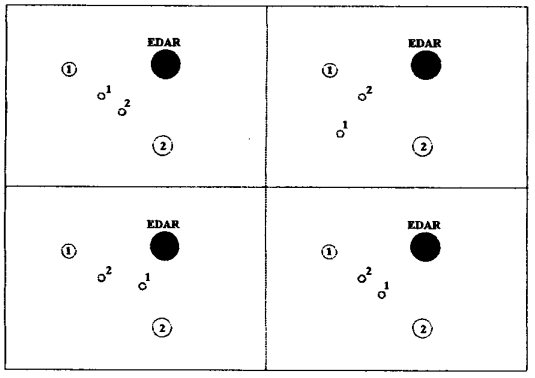

Figure 6 2D projections of 2-part parts' moving of increasing difficulty: i) *erc=0.487*, ii) *erc=1.100*, iii) *erc=1.617*, iv) *erc=2.631*.

Two measures are used for EDAR motion: 1) normalized path length of EDAR *nrl*, 2) normalized part path length *npl*. The path length of EDAR is the total distance travelled. In order to account for variations in the initial configurations, it is normalized by the total Euclidean distance between the points visited by the robot. It is defined as:

$$nrl = \frac{2\int_{t_i}^{t_f} r\,dt}{\|r(0) - p_1(0)\| + \|p(0) - d\| + \|d_1 - p_2(0)\|}$$

where t_i, t_f are the starting and ending time of the task, d represents the destination coordinates of the parts and $p(0)$ represents initial position vector of the parts. The parts' path length is distance travelled by parts. In order to account for variations in the initial configurations, it is normalized by the Euclidean distance between the initial and the final configurations. It is defined as:

$$npl = \frac{\int_{t_i}^{t_f} p\,dt}{\|d - p(0)\|}$$

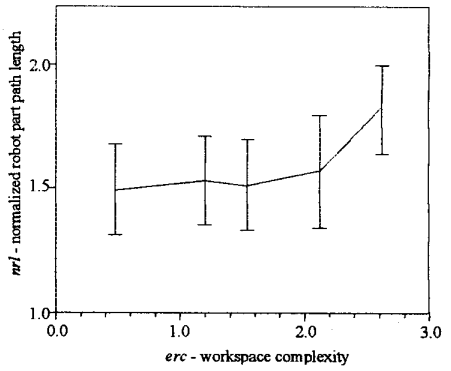

Figure 7 Normalized robot path length statistics.

Normalized Robot Path Length vs. Complexity

Figure 7 shows that the normalized path length of EDAR increases with increasing workspace complexity. The more complex the parts' moving task is, EDAR travels a longer distance. Interestingly, this result is in agreement to those of similar statistics in simulations of [8]. EDAR has a reasonable velocity (~ 6 cm/sec) comparing to workspace dimensions and it completes two parts' moving in two to four minutes according to the workspace complexity. The average distance between the parts is about 1.5 meter in all configurations. In simple workspaces, the absolute robot path length becomes 2 times the Euclidean distance between the two parts whereas in difficult workspaces, this ratio becomes 2.5 times. So, EDAR travels %25 more path in more complex workspaces compared to the simple ones.

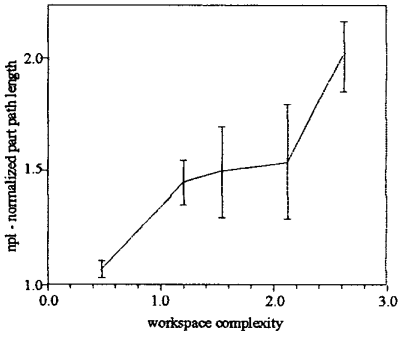

Figure 8 Normalized part path length statistics.

Normalized part path length vs. workspace complexity

Figure 8 shows the relation between the workspace complexity and the travelled distance by the parts. As expected, the travelled distance by the parts increase when

the workspace complexity increases. The workspace complexity corresponds to the alignment of the parts and their destinations. If the second part is between the first part and its destination, *npl* increases because the second part travels more distance to go to its destination. That behaviour of normalized path length statistics is parallel with the results of [8]. We further note that variation of the npl is relatively less in the least and most complex configurations as compared to the tasks with intermediate complexity.

5 Conclusion

These EDAR experiments offer a realistic picture of how an event-driven approach to parts' motion might be realized in conventional assembly settings. The robot- whose actuator commands are automatically generated using a feedback scheme - moves a set of parts parts from an arbitrary initial disassembled configuration to a specified final configuration. Our experiments validate our former findings that an alternative approach to parts' moving problem may be based on a composite algorithm that reactively switches between different feedback controllers.

Acknowledgements

This research is supported by the NSF under grant INT-9819890. The first two authors have been supported in part by TÜBİTAK MİSAG 65-1995 and Boğaziçi University Fund #99HA201. The third author has been supported in part by the NSF under grant 9510673. We gratefully acknowledge the contributions and assiduous work of İhsan Hoşver to mechanical design and implementation.

References

1. Lozano-Perez, T., J.L Jones, E. Mazer., P.A. O'Donell, and W.E.L. Grimson. Handey: A Robot System that Recognizes, Plans and Manipulates. In *Proceedings of IEEE Int. Conference on Robotics and Automation*, pp. 843-849, 1987.
2. Garibotto G., S. Masciangelo, M. Ilic, and P. Bassino. Service Robotics in Logistic Automation: ROBOLIFT: Vision Based Autonomous Navigation of a Conventional Fork-Lift for Pallet Handling. In *International Conference of Advanced Robotics*, pp. 781-785, July, 1997.
3. Min B., D.W. Cho, S. Lee, and Y. Park. Sonar Mapping of a Mobile Robot Considering Position Uncertainty. *Robotics and Computer-Integrated Manufacturing*, Vol. 13, No. 1, pp. 41-49, 1997.
4. Cha Y.Y., and D.G. Gweon. Local Path Planning of a Free Ranging Mobile Robot Using the Directional Weighting Method. *Mechatronics* , Vol. 6, No. 1, pp. 53-80, 1996.
5. Whitcomb L.L., D.E. Koditschek, and J.B.D.Cabrera. Toward the Automatic Control of Robot Assembly Tasks via Potential Functions: The Case of 2D Sphere Assemblies. In *Proceedings of IEEE Int. Conference on Robotics and Automation*, 1992.
6. Bozma, H.I. and D.E. Koditschek. Assembly as a Noncooperative Game of its Pieces: Analysis of 1D Sphere Analysis. *Paper in preparation.*
7. Yalçın H. and I. Bozma, "An Automated Inspection System with Biologically Inspired Vision," *Proceedings of IROS'98*, 3:1808-1814.
8. Bozma H.I., C.S. Karagöz, and D.E. Koditschek. Assembly as a Noncooperative Game of its Pieces: The Case of Endogenous Disk Assemblies. In *Proceedings of IEEE Int. Symposium on Assembly and Task Planning*, pp:2-8, Pittsburg, PA, 1995.
9. SMART EYE I, User's Manual. VISIONEX, INC. Revision C, February 1995.
10. Koditschek, D.E. An approach to autonomous robot assembly. *Robotica*, 12: 137-155, 1994.
11. Koditschek, D.E. and E. Rimon. Robot navigation functions on manifolds with boundary. *Advances in Applied Mathematics*, 11: 412-442, 1992.
12. Soyer, Ç., H.I. Bozma and Y. İstefanopulos. A Mobile Robot With a Biologically Motivated Vision System. In *Proceedings of the 1996 IEEE/RSJ Int. Conference on Intelligent Robots and Systems*, pp:680-687, Osaka, Japan 1996.
13. Ballard, D.H and C.M. Brown. Principles of Animate Vision. *CVIP: Image Understanding*, 56(1), July 1992.
14. Bozma, H.I. and D.E. Koditschek, "Assembly as a Noncooperative Game of its Pieces: Analysis of 1D Sphere Assemblies", (to appear) Robotica, 1999.
15. Proceedings of IEEE International Symposium on Assembly and Task Planning, Pittsburg, PA, August 1995.
16. Ames, A.L., T.E. Calton, R.E. Jones, S.G. Kaufman, C.A. Laguna, R.H. Wilson. "Lessons Learned from a Second Generation Assembly Planning System", Proceedings of IEEE International Symposium on Assembly and Task Planning, Pittsburg, PA, August 1995.
17. Hemmingson, Eric. Palletizing Robot for The Consumer Goods Industry. *Industrial Robot*, Volume 25, Number 6, pp: 384-388, 1998.
18. Motoman Introduces New SP100 Robot: Ideal Manipulator for High-speed, Heavy Palletizing. *Industrial Robot*, Volume 25, Number 2, pp: 148, 1998.
19. http://www.fanucrobotics.com.